Relativistic Impulse Approximation for p-Nucleus Elastic Scattering

J. R. Shepard
Department of Physics, University of Colorado, Boulder, Colorado 80309

and

J. A. McNeil
Department of Physics, Villanova University, Villanova, Pennsylvania 19085, and Department of Physics, University of Pennsylvania, Philadelphia, Pennsylvania 19104

and

S. J. Wallace
Department of Physics and Astronomy, University of Maryland, College Park, Maryland 20742

(Received 17 February 1983)

First calculations based on an impulse-approximation Dirac optical potential are presented. All input parameters are constrained by other experimentally determined quantities. Excellent agreement with $T_p = 500$ MeV $p_{\rm pol}$ + ^{16}O and ^{40}Ca elastic scattering data is demonstrated. The differences between the relativistic and nonrelativistic results are explored in detail.

PACS numbers: 24.10.Ht, 25.40.Cm

As Dirac showed over fifty years ago, the spin-$\frac{1}{2}$ character of electrons is intimately linked with relativity. Nucleons, although not fundamental Dirac particles, can usually be treated as such to good approximation. Over the past few years, an essentially phenomenological Dirac potential for proton-nucleus elastic scattering has been developed.[1-3] Strong scalar and fourth-component vector potentials in the Dirac equation provide an economical picture of many of the features of the scattering process. While it has been known for some time that the real parts of these potentials are qualitatively consistent with the relativistic one-boson–exchange description of NN scattering[4] and with measured nuclear densities,[5] a quantitative understanding of them is just beginning to emerge. In the energy range below ≈ 200 MeV, it has been shown[6,7] that the phenomenological potential strengths are consistent with nucleon self-energies calculated with use of relativistic models of infinite nuclear matter. Recently, we have derived an expression for an impulse approximation, or "$t\rho$," Dirac optical potential and have found[8] the strengths of these potentials to be qualitatively consistent with phenomenology for bombarding energies above ≈ 200 MeV.

In the present paper, we present the first intermediate-energy p-nucleus elastic scattering calculations based on the relativistic $t\rho$ potential of Ref. 8. As will be discussed below, all input parameters are fixed by other experimentally determined quantities and consequently comparison with the extensive data which are available constitutes a particularly informative test of the Dirac approach.

The specific processes we have examined are the elastic scattering of protons from the spin-saturated nuclei ^{16}O and ^{40}Ca at energies between 181 and 800 MeV. It is interesting to note that the 500-MeV $p_{\rm pol}$ + ^{40}Ca data pose a significant problem for nonrelativistic multiple-scattering theories. For example, Hoffmann *et al.*[9] encountered difficulty in reproducing the analyzing-power data with refined Kerman-McManus-Thaler calculations[10] and suggested this as evidence of a breakdown of the impulse approximation at 500 MeV. Subsequent calculations by Barlett, Hoffmann, and Ray[11] have shown that use of medium-modified density-dependent t matrices improves the situation only slightly.

The Dirac optical potential used in the present calculations is given by[8]

$$\langle \vec{p}' | U_{00} | \vec{p} \rangle = -\frac{4\pi i p}{m} \Psi_0^{\dagger} \sum_{i=1}^{A} \gamma^0(i) \sum_{\lambda} F_{\lambda}(p, i) \Psi_0, \quad (1)$$

where m is the nucleon mass, p is the projectile-target center-of-momentum frame three-momen-

tum, Ψ_0 is the (relativistic) target ground state, and

$$\sum_\lambda F_\lambda(1,2) = F_S + \gamma(1)\cdot\gamma(2)F_V + \gamma^5(1)\gamma^5(2)F_P + \gamma^5(1)\gamma^5(2)\gamma(1)\cdot\gamma(2)F_A + \sigma_{\mu\nu}(1)\sigma^{\mu\nu}(2)F_T \quad (2)$$

is the relativistic form of the *NN* invariant amplitude.[8,12] If we assume a spin-saturated target, the nuclear matrix element shown in Eq. (1) implies a trace over the spin of one of the nucleons in Eq. (2). Upon also assuming a local form for the F's, we obtain, in momentum space, the scalar and vector potentials

$$U_{00}(q) = (-4\pi i p/m)[F_S(q)\rho_S(q) + \gamma^0 F_V(q)\rho_V(q)],$$

where ρ_S and ρ_V are scalar and (fourth-component) vector densities, respectively. If we assume Ψ_0 to be a product wave function, these densities can be written in configuration space in terms of the target single-particle wave functions as follows:

$$\rho_S(r) = \sum_{i=1}^{A} \Psi_0{}^\dagger \gamma_0(i)\delta(\vec{r} - \vec{r}_i)\Psi_0$$

$$= \rho_\uparrow(r) - \rho_\downarrow(r), \quad (3a)$$

$$\rho_V(r) = \sum_{i=1}^{A} \Psi_0{}^\dagger \delta(\vec{r} - \vec{r}_i)\Psi_0 = \rho_\uparrow(r) + \rho_\downarrow(r), \quad (3b)$$

where

$$\rho_\uparrow(r) \equiv \sum_{i=1}^{A} |u_i|^2, \quad \rho_\downarrow(r) \equiv \sum_{i=1}^{A} |w_i|^2 \quad (3c)$$

are the large- and small-component densities, respectively. Note that the vector density is the probability density and that elastic electron scattering constrains the vector density of the protons. The scalar density has no nonrelativistic analog. For nuclei it is approximately equal to the vector density.

Our relativistic *NN* invariant amplitude is determined from *NN* phase shifts[13] as described in Ref. 12. Simple Yukawa functions are used to parametrize the q dependence with separate strengths and ranges for the real and imaginary parts. These amplitudes are consistent with the notion that the *NN* force is characterized by a strong intermediate-range attraction (σ meson) and short-range repulsion (ω meson). The densities of Eq. (3) which we use are based on relativistic single-particle wave functions which are consistent with elastic electron scattering. The single-particle wave functions used give the phenomenological single-particle binding energies and a proton vector density which, when folded with a phenomenological proton charge distribution,[14] is consistent with $e^- + {}^{40}$Ca elastic scattering data.[15] The bound-state Dirac potentials are consistent with the real parts of phenomenological low-energy $p + {}^{40}$Ca Dirac optical potentials.[2] Following this procedure, we generate neutron densities and a proton scalar density which are consistent with the phenomenologically determined proton vector density. The small-component densities [Eq. (3c)] account for about 2% of the total probability.

The Dirac equation containing the resulting optical potential from Eq. (3) was solved numerically. Calculated values of the cross section, the analyzing power, and the spin-rotation parameter, Q, are compared with 500-MeV $p_{\rm pol} + {}^{40}$Ca data[9,16] in Fig. 1. The agreement is extraordinary for a theoretically based calculation, especially for the spin observables. It is comparable to a phenomenological analysis[17] and definitely superior to the nonrelativistic impulse-approximation calculations of Refs. 9 and 11. Similar agreement is found for 500-MeV $p_{\rm pol} + {}^{16}$O analyzing-power data.[18] At 800 MeV, the agreement with the ^{40}Ca data[16] is also very good, if perhaps not so extraordinary as that shown in Fig. 1. At 181 MeV, the calculations reproduce the data[3] only qualitatively, suggesting that the impulse approximation may be appreciably poorer at that energy.

It is of course crucial to understand which ingredients of the relativistic calculations are responsible for the improvement over the nonrelativistic results. We recall that the Dirac equation containing scalar and fourth-component vector potentials can be reduced without approximation to the form of a Schrödinger equation containing effective central and spin-orbit potentials. Using the usual nonrelativistic expressions for the $t\rho$ optical potential[19] and the formulas given in Ref. 12 for the central and spin-orbit *NN* amplitudes, $A_{\rm lab}$ and $C_{\rm lab}$, in terms of the relativistic invariants, F_λ, we can directly compare the relativistic and nonrelativistic potentials. (In the following we ignore small contributions to $C_{\rm lab}$ from F_A and F_T.) For the configuration-space central potentials we find, again ignoring Coulomb and

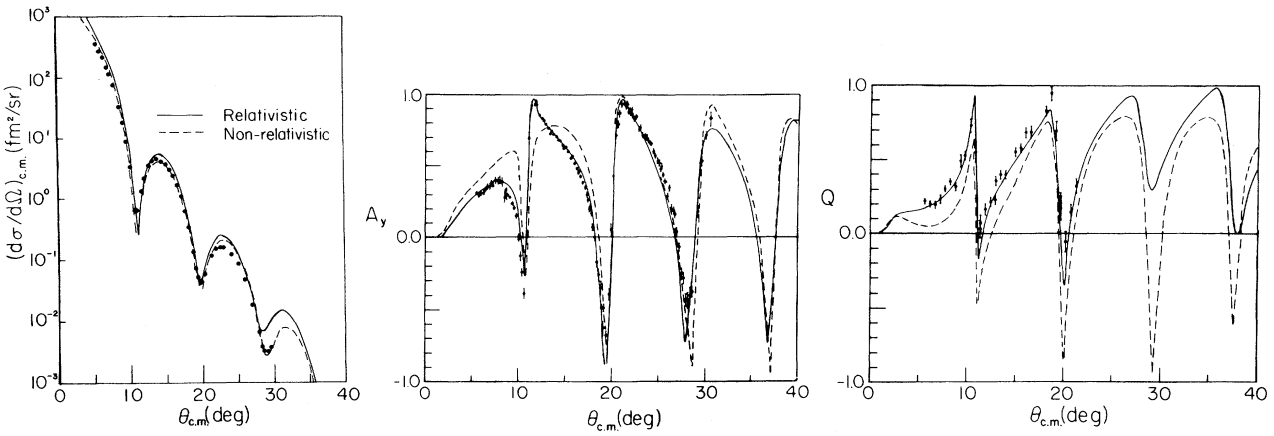

FIG. 1. Data for $p + {}^{40}$Ca elastic scattering at $T_p = 500$ MeV compared with full relativistic (solid line) and nonrelativistic (dashed line) $t\rho$ calculations. The nonrelativistic calculations employ a form of the NN t matrix which explicitly contains the ranges of the scalar and vector contributions (see text for explanation).

$1/A$ effects,

$$V_{\text{cent}}^{\text{NR}} = -4\pi i[(p/E)F_S(0) + (p/m)F_V(0)]\rho_{\text{cent}}(r), \tag{4a}$$

$$V_{\text{cent}}^{\text{R}} = -4\pi i[(p/E)F_S(0)\rho_{\text{scal}}(r) + (p/m)F_V(0)\rho_{\text{vect}}(r)] + (V_S^2 - V_V^2)/2E + V_{\text{Darwin}}, \tag{4b}$$

where V_S and V_V are the scalar and vector potentials constituting the first two terms of Eq. (4b) and the explicit form of the Darwin term is given by Rost, Shepard, and Murdock.[20] The subscripts on the densities indicate that the appropriate point density is folded over the range of the relevant *NN* interaction. For example, $\rho_{\text{cent}}(r)$ is obtained by folding the vector point density, ρ_V, over the range of A_{lab}. The spin-orbit potentials are

$$V_{\text{s.o.}}^{\text{NR}} = +2\pi i \frac{p}{Em(E+m)}[F_S(0) - F_V(0)]\frac{1}{r}\frac{d}{dr}\rho_{\text{s.o.}}(r), \tag{5a}$$

$$V_{\text{s.o.}}^{\text{R}} = +2\pi i \frac{p}{Em(E+m)} B^{-1}(r)\frac{1}{r}\frac{d}{dr}[F_S(0)\rho_{\text{scal}}(r) - F_V(0)\rho_{\text{vect}}(r)], \tag{5b}$$

where $B = 1 - (V_V - V_S)/(E+m)$.

The relativistic effective central potential differs from its nonrelativistic counterpart by quadratic and Darwin terms. Also, the scalar density enters only in the relativistic potentials. Beyond this, however, the differences are subtle geometrical ones. For example, the relativistic spin-orbit potential contains an extra factor, $B^{-1}(r)$, which enhances the spin-orbit strength in the nuclear interior just as the small components of the projectile wave function are enhanced as a result of the strong vector and scalar optical potentials.[21] This is consistent with the fact that, relativistically, the spin-orbit interaction originates with the small components. Equations (4) and (5) also indicate that the folding of the *NN* interaction with the nuclear density is done differently in the two cases. In principle, such a distinction should be irrelevant, since the same information is contained in both the relativistic and the nonrelativistic forms of the phenomenological *NN* amplitude. However, in practice, when the *NN* amplitude is approximated by convenient functional forms such as the Yukawa functions used here, some information is lost and details of the folding procedures can be important. This is most pronounced for the central potential where there is a great deal of cancellation between the vector and scalar contributions.

Nonrelativistic calculations where folding is done over A_{lab} and C_{lab} with real and imaginary parts parametrized as single Yukawa functions are in very poor agreement with the spin observables. In contrast, nonrelativistic calculations using the relativistic form of the *NN* amplitude (represented by the dashed curves in Fig. 1) are in much better accord with experiment. Here A_{lab} is taken to be the appropriate (algebraic) sum[12] of F_S and F_V therefore becomes the dif-

ference of Yukawa functions. Similarly C_{1ab} is treated as the appropriate[12] difference of F_S and F_V which corresponds to the sum of Yukawa functions. Although in better agreement with the analyzing-power data, the present nonrelativistic calculations are less accurate than the optical-model results of Ref. 9 which incorporate folding over the exact *NN* amplitude and include second-order terms.

By construction, the calculations shown in Fig. 1 employ identical forms of the *NN* interaction. Therefore the differences between the solid and dashed curves can be attributed entirely to relativistic effects. The uniquely relativistic Darwin potential has long been known to have little influence on elastic scattering[1] and we reach the same conclusion here. However, the remaining relativistic features, the B^{-1} factor in the effective spin-orbit potential [Eq. (5b)], the quadratic terms in the effective central potential [Eq. (4b)], and the nonzero difference between ρ_S and ρ_V [Eq. (3c)], are about equally responsible for the differences between the dashed and solid curves in Fig. 1. Note that the B^{-1} factor increases the strength of the effective spin-orbit potential in the nuclear interior, consistent with the finding by Hoffmann *et al.*[9] that arbitrarily increasing ImC in nonrelativistic calculations results in improved agreement with the forward-angle analyzing-power data. The fact that the difference between ρ_S and ρ_V has an appreciable effect on the calculated spin observables is potentially exciting because this difference depends on the small components of the target nucleons [Eq. (3c)]. The suggestion[3] that it may eventually be feasible to learn about the relativistic properties of nuclear wave functions through nucleon-nucleus elastic scattering measurements is now a definite possibility.

The impulse-approximation Dirac optical potential excels in predicting the spin observables for $p_{pol}+{}^{16}$O and ^{40}Ca elastic scattering at $T_p = 500$ MeV. This is in marked contrast to the standard nonrelativistic approaches which fail to account for these data. Our calculations emphasize again the essential role that relativity plays in understanding spin.

The assistance of D. Murdock in performing the calculations is gratefully acknowledged, as is the financial support of the U. S. Department of Energy.

[1]L. G. Arnold *et al.*, Phys. Rev. C 25, 936 (1982), and references contained therein.
[2]L. G. Arnold and B. C. Clark, Phys. Lett. 84B, 46 (1979).
[3]L. G. Arnold *et al.*, Phys. Rev. C 23, 1949 (1981).
[4]K. Holinde, Phys. Rep. 68, 121 (1981), and references contained therein.
[5]C. W. Jaeger, H. Devries, and C. Devries, At. Nucl. Data Tables 14, 479 (1974).
[6]C. Horowitz, Phys. Lett. 117, 153 (1982), and in Proceedings of the Indiana University Cyclotron Facility Workshop, October 1982 (unpublished), and to be published.
[7]C. M. Shakin, in Proceedings of the Indiana University Cyclotron Facility Workshop, October 1982 (unpublished), and to be published.
[8]J. A. McNeil, J. R. Shepard, and S. J. Wallace, preceding Letter [Phys. Rev. Lett. 50, 1439 (1983)], and to be published.
[9]G. W. Hoffmann *et al.*, Phys. Rev. Lett. 47, 1436 (1981).
[10]L. Ray, Phys. Rev. C 19, 1855 (1979).
[11]M. L. Barlett, G. W. Hoffmann, and L. Ray, Bull. Am. Phys. Soc. 27, 729 (1982).
[12]J. A. McNeil, L. Ray, and S. J. Wallace, University of Maryland Report No. 83-097 (to be published), and to be published.
[13]S. J. Wallace, in *Advances in Nuclear Physics*, edited by J. W. Negele and E. Vogt (Plenum, New York, 1981), Vol. 12, p. 135.
[14]F Borkowski *et al.*, Nucl. Phys. A222, 269 (1974).
[15]B. Bellicard *et al.*, Phys. Rev. Lett. 19, 527 (1967).
[16]G. W. Hoffmann, private communication.
[17]B. C. Clark, R. L. Mercer, and P. Schwandt, Phys. Lett. 122B, 211 (1983).
[18]M. Hynes, private communication.
[19]A. K. Kerman, H. McManus, and R. M. Thaler, Ann. Phys. (N.Y.) 8, 551 (1959).
[20]E. Rost, J. R. Shepard, and D. Murdock, Phys. Rev. Lett. 49, 448 (1982).
[21]J. R. Shepard, in Proceedings of the Indiana University Cyclotron Facility Workshop, October 1982 (unpublished), and to be published.